

# Exact artificial boundary conditions for problems with periodic structures

Matthias Ehrhardt<sup>a,\*</sup>, Chunxiong Zheng<sup>b,1</sup>

<sup>a</sup> Weierstrass Institute for Applied Analysis and Stochastics, Mohrenstrasse 39, 10117 Berlin, Germany

<sup>b</sup> Department of Mathematical Sciences, Tsinghua University, Beijing 100084, PR China

Received 27 July 2007; received in revised form 6 March 2008; accepted 31 March 2008

Available online 12 April 2008

---

## Abstract

Based on the work of Zheng on the artificial boundary condition for the Schrödinger equation with sinusoidal potentials at infinity, an analytical impedance expression is presented for general second-order ODE problems with periodic coefficients and its validity is shown to be strongly supported by numerical evidences. This new expression for the kernel of the Dirichlet-to-Neumann mapping of the artificial boundary conditions is then used for computing the bound states of the Schrödinger operator with periodic potentials at infinity. Other potential applications are associated with the exact artificial boundary conditions for some time-dependent problems with periodic structures. As an example, a two-dimensional hyperbolic equation modeling the TM polarization of the electromagnetic field with a periodic dielectric permittivity is considered.

© 2008 Elsevier Inc. All rights reserved.

MSC: 65M99; 81–08

Keywords: Artificial boundary conditions; Periodic potential; Schrödinger equation; Hyperbolic equation; Unbounded domain

---

## 1. Introduction

Periodic structure problems largely exist in the science and engineering and often they are modeled by partial differential equations with periodic coefficients and/or periodic geometries. In order to numerically solve these equations efficiently one usually confines the spatial domain to a bounded computational domain (in a neighborhood of the region of physical interest). The usual strategy is to introduce so-called *artificial boundaries* and impose adequate boundary conditions. For wave-like equations, the ideal boundary conditions should not only lead to well-posed problems, but also mimic the perfect absorption of waves traveling out

---

\* Corresponding author. Tel.: +49 30 20372332; fax: +49 30 2044975.

E-mail addresses: [ehrhadt@wias-berlin.de](mailto:ehrhadt@wias-berlin.de) (M. Ehrhardt), [czheng@math.tsinghua.edu.cn](mailto:czheng@math.tsinghua.edu.cn) (C. Zheng).

URLs: <http://www.wias-berlin.de/~ehrhadt/> (M. Ehrhardt), <http://faculty.math.tsinghua.edu.cn/czheng/> (C. Zheng).

<sup>1</sup> Supported by the Alexander-von-Humboldt Foundation and the National Natural Science Foundation of China under Grant No. 10401020.

of the computational domain through the artificial boundaries. Right in this context, these boundary conditions are usually called *artificial* (or transparent, non-reflecting in the same spirit) in the literature. The interested reader is referred to a couple of review papers [2,11,12,24] on this research topic.

Artificial boundary conditions (ABCs) for the Schrödinger equation and related problems has been a hot research topic for many years [2]. Since the first exact ABC for the Schrödinger equation was derived by Papadakis [16] 25 years ago, many developments have been made on the designing and implementing of various ABCs, also for multi-dimensional and nonlinear problems. However, the question of exact ABCs for periodic structures still remained open, and it is a very up-to-date research topic, cf. the current papers [8–10,13,21–23,26,27]. These kind of new ABCs can be applied in many physical problems, e.g. in optical applications from micro and nano-technology [15,20] and *semiconductor superlattices*. We refer to the book from Bastard [4] or the review by Wacker [25] for more details on superlattice transport modelling.

Very recently, Zheng [29] derived exact ABCs for the Schrödinger equation of the form

$$iu_t + u_{xx} = V(x)u, \quad x \in \mathbb{R}, \quad (1a)$$

$$u(x, 0) = u_0(x), \quad x \in \mathbb{R}, \quad (1b)$$

$$u(x, t) \rightarrow 0, \quad x \rightarrow \pm\infty. \quad (1c)$$

The initial function  $u_0 \in L^2(\mathbb{R})$  is assumed to be compactly supported in an interval  $[x_L, x_R]$ , with  $x_L < x_R$ , and the real potential function  $V \in L^\infty(\mathbb{R})$  is supposed to be sinusoidal on  $(-\infty, x_L]$  and  $[x_R, +\infty)$ . It is well-known that the system (1a) has a unique solution  $u \in C(\mathbb{R}^+, L^2(\mathbb{R}))$  (cf. [17,18], e.g.):

**Theorem 1.** *Let  $u_0 \in L^2(\mathbb{R})$  and  $V \in L^\infty(\mathbb{R})$ . Then the system (1a) has a unique solution  $u \in C(\mathbb{R}^+, L^2(\mathbb{R}))$ . Moreover, the “energy” is preserved, i.e.*

$$\|u(\cdot, t)\|_{L^2(\mathbb{R})} = \|u_0\|_{L^2(\mathbb{R})}, \quad \forall t \geq 0.$$

More precisely, Zheng [29] assumed

$$V(x) = V_L + 2q_L \cos \frac{2\pi(x_L - x)}{S_L}, \quad \forall x \in (-\infty, x_L],$$

$$V(x) = V_R + 2q_R \cos \frac{2\pi(x - x_R)}{S_R}, \quad \forall x \in [x_R, +\infty),$$

where  $S_L$  and  $S_R$  are the periods,  $V_L$  and  $V_R$  are the average potentials, and the nonnegative numbers  $q_L$  and  $q_R$  relate to the amplitudes of sinusoidal part of the potential function  $V$  on  $(-\infty, x_L]$  and  $[x_R, +\infty)$ , respectively. Let us note that Galicher [10] also considered the same problem but with a general periodic potential. Formally he set up at each artificial boundary point an exact Dirichlet-to-Dirichlet mapping, which is nonlocal in both time and space.

The organization of the paper is as follows. In Section 2, we conjecture an elegant analytical expression of the impedance operator for general periodic problems and present an exact ABC in a form of Dirichlet-to-Neumann mapping. In Section 3 we use this result to compute bound states for the Schrödinger operator. Finally, in Section 4 we show how the results can be generalized to the time-dependent Schrödinger equation, a diffusion equation and a second-order hyperbolic equation and present a concise numerical example.

## 2. A conjecture on the impedance expression

Let us start with the following *general second-order ODE*

$$-\frac{d}{dx} \left( \frac{1}{m(x)} \frac{dy}{dx} \right) + V(x)y = \rho(x)zy, \quad \forall x \geq 0, \quad (2)$$

where  $z$  denotes a complex parameter whose value space is to be determined. We assume that the functions  $m(x)$ ,  $V(x)$  and  $\rho(x)$  are all  $S$ -periodic in  $[0, +\infty)$  and *centrally symmetric* in each period, i.e.,

$$m(x) = m(S - x), \quad V(x) = V(S - x), \quad \rho(x) = \rho(S - x), \quad a.e. x \in [0, S]. \quad (3)$$

The symmetry condition (3) simply implies that the *even* extensions of these functions to the whole real axis are still  $S$ -periodic. Moreover, we assume that the functions  $m(x)$ ,  $V(x)$  and  $\rho(x)$  are sufficiently smooth and bounded, i.e. there exist several constants  $M_0, M_1, V_0$  and  $\rho_0$ , such that

$$0 < M_0 \leq m(x) \leq M_1 < +\infty, \quad V(x) \geq V_0, \quad \rho(x) \geq \rho_0 > 0, \quad \forall x \in [0, S].$$

By introducing the new variable

$$w = \frac{1}{m(x)} \frac{dy}{dx},$$

the second-order ODE (2) is transformed into a *first-order ODE system*

$$\frac{d}{dx} \begin{pmatrix} w \\ y \end{pmatrix} = \begin{pmatrix} 0 & V(x) - \rho(x)z \\ m(x) & 0 \end{pmatrix} \begin{pmatrix} w \\ y \end{pmatrix}, \quad \forall x \geq 0. \tag{4}$$

This paper is concerned with the  $L^2$ -solution of (2) in  $[0, +\infty)$ . More precisely, we would like to know for what  $z$  the ODE (2) possess an  $L^2$ -solution  $y(x)$ , and in this case what is the impedance  $I := y'(0)/y(0)$ , namely the quotient of Neumann data over Dirichlet data evaluated at  $x = 0$ .

For any two points  $x_1$  and  $x_2$ , the ODE system (4) uniquely determines a linear transformation from the two-dimensional vector space associated with  $x_1$ , to the same space associated with  $x_2$ . We identify this transformation with the  $2 \times 2$  matrix  $T(x_1, x_2)$ , which satisfies the same form of equation as (4), namely:

$$\frac{d}{dx} T(x_1, x) = \begin{pmatrix} 0 & V(x) - \rho(x)z \\ m(x) & 0 \end{pmatrix} T(x_1, x), \quad \forall x_1 \geq 0, \quad \forall x \geq 0. \tag{5}$$

This *transformation matrix*  $T$  satisfies the following properties:

$$T(x, x) = I_{2 \times 2}, \quad \det T(x_1, x_2) = \det T(x_1, x_1) = 1, \tag{6a}$$

$$T(x_2, x_3)T(x_1, x_2) = T(x_1, x_3), \tag{6b}$$

$$T(x_1 + S, x_2 + S) = T(x_1, x_2). \tag{6c}$$

According to (6a), the matrix  $T(0, S)$  has two eigenvalues  $\sigma (\neq 0)$  and  $1/\sigma$  with  $|\sigma| \leq 1$ . Their associated eigenvectors are denoted by  $(c_+, d_+)^T$  and  $(c_-, d_-)^T$ . If  $|\sigma| < 1$ , then  $T(0, x)(c_\pm, d_\pm)^T$  yields two linearly independent solutions of the ODE system (4). By setting  $\sigma = e^{\mu S}$  with  $\text{Re} \mu < 0$  it is straightforward to verify that  $e^{\mp \mu x} T(0, x)(c_\pm, d_\pm)^T$  are periodic functions. Therefore, we conclude that

$$y_+ := T(0, x)(c_+, d_+)^T = e^{\mu x} e^{-\mu x} T(0, x)(c_+, d_+)^T$$

is  $L^2$ -bounded, while

$$y_- := T(0, x)(c_-, d_-)^T = e^{-\mu x} e^{\mu x} T(0, x)(c_-, d_-)^T$$

is not. For the  $L^2$ -bounded solution  $y_+$ , the impedance  $I$  is thus given as

$$I := \frac{y_+'(0)}{y_+(0)} = m(0) \frac{c_+}{d_+}. \tag{7}$$

We remark that  $\sigma$  and  $(c_+, d_+)^T$  depend on  $z$ , and hence the impedance  $I$  also depends on  $z$ . In the sequel we will refer to  $\sigma$  as the *Floquet's factor* [3,14,19]. It typically reflects how fast the  $L^2$ -bounded solution of the ODE (2) decays to zero when  $x$  tends to  $+\infty$ : the smaller its modulus, the faster. Also note that  $\sigma(\bar{z}) = \overline{\sigma(z)}$  and  $I(\bar{z}) = \overline{I(z)}$  holds. The impedance (7) is computed after  $T(0, S)$  is obtained (cf. the impedance plots in Figs. 5 and 6 for some values of  $z$ ).

In general, the matrix  $T(0, S)$  cannot be represented with a simple analytical expression in terms of the functions  $m(x)$ ,  $V(x)$  and  $\rho(x)$ . However, it can be computed sufficiently accurately by integrating the ODE (5) (setting  $x_1 = 0$ ) in the interval  $[0, S]$  with the initial data  $T(0, 0) = I_{2 \times 2}$ . Since this task is a standard issue, the detailed discussion is omitted here.

We consider in the sequel three cases:

- Case A :**  $m(x) = \rho(x) = 1, \quad V(x) = 2 \cos(2x);$
- Case B :**  $m(x) = \rho(x) = 1 + \cos(2x)/5, \quad V(x) = \cos(2x);$
- Case C :**  $m(x) = \rho(x) = 1 + \cos(2x)/5, \quad V(x) = \sin(2x).$

Figs. 1–3 show the modulus of  $\sigma$ , which denotes the eigenvalue of  $T(0, S)$  with a smaller modulus. We observe that apart from some intervals in the real axis, for any  $z$  in the complex plane,  $\sigma$  has a modulus less than 1, thus the second-order ODE (2) has a nontrivial  $L^2$ -solution. Furthermore, it turns out that the ending points of these intervals are exactly the eigenvalues of the following *characteristic problem*:

Find  $\lambda \in \mathbb{R}$  and a nontrivial  $y \in C_{\text{per}}^1[0, 2S]$ , such that

$$-\frac{d}{dx} \left( \frac{1}{m(x)} \frac{dy}{dx} \right) + V(x)y = \rho(x)\lambda y. \tag{8}$$

We note that the symmetry condition (3) is not necessary for the above statements (in fact Case C does not satisfy (3)). We admit that the above statements have not been proven up to this time, but a vast number of other numerical evidences also support their validity.

If the coefficient functions  $m(x)$ ,  $V(x)$  and  $\rho(x)$  satisfy the symmetry condition (3), then the characteristic problem (8) has a nice property: all the eigenvalues can be classified into two different groups

$$a_1 < a_2 < a_3 < \dots \quad \text{and} \quad b_1 < b_2 < b_3 < \dots,$$

where the eigenvalues  $a_r$  are associated with even eigenfunctions, and  $b_r$  with odd eigenfunctions. Besides, it holds that

$$a_1 < \min(a_2, b_1) \leq \max(a_2, b_1) < \min(a_3, b_2) \leq \max(a_3, b_2) < \dots$$

For the Schrödinger equation (SE) with a periodic cosine potential, a special case of (2) with  $m(x) = \rho(x) = 1$  and  $V(x) = 2q \cos(2x)$ , the second author [29] made a conjecture upon the impedance expression

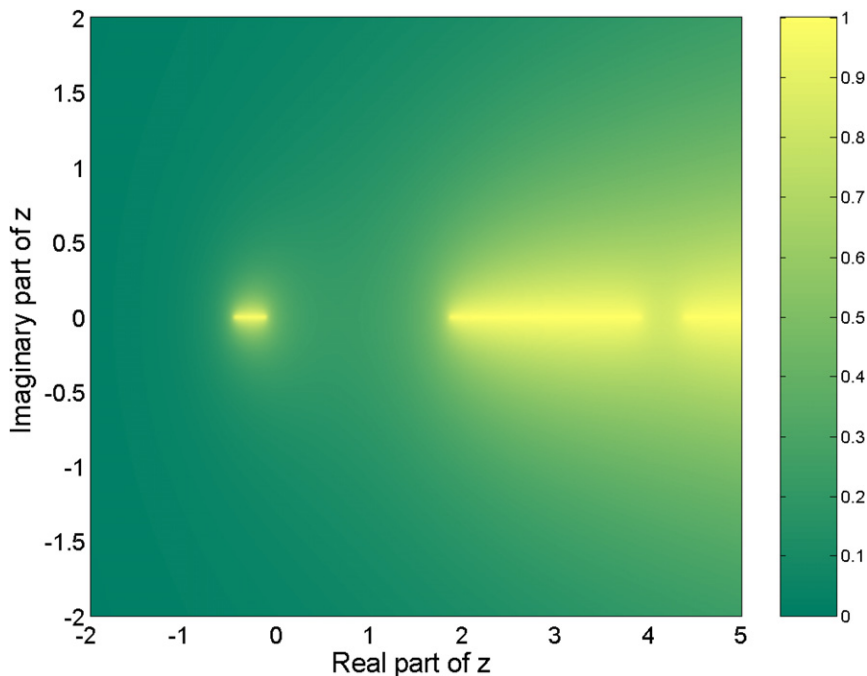


Fig. 1. Case A: Modulus of  $\sigma$  with respect to  $z$ .

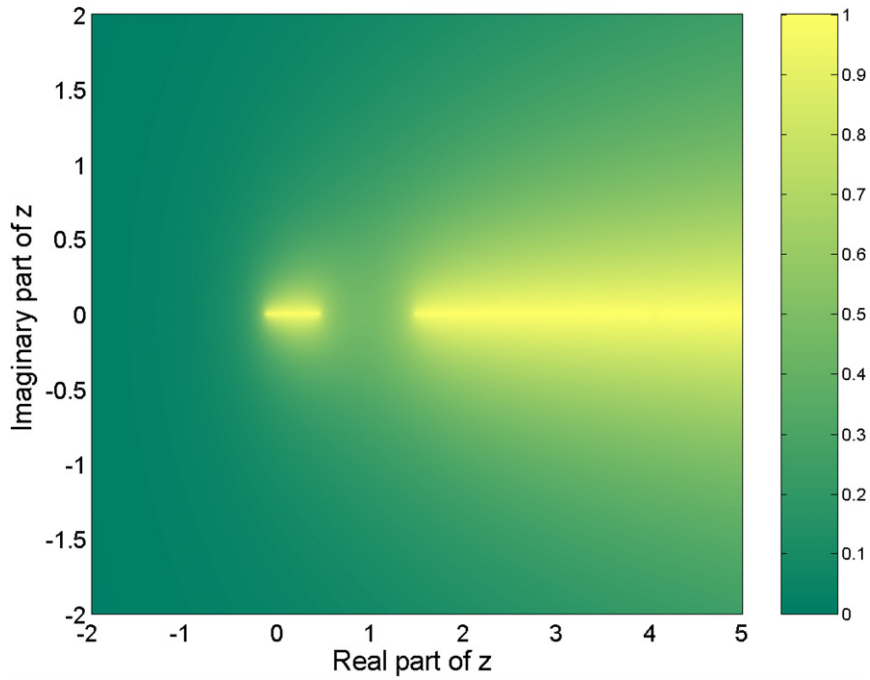


Fig. 2. Case B: Modulus of  $\sigma$  with respect to  $z$ .

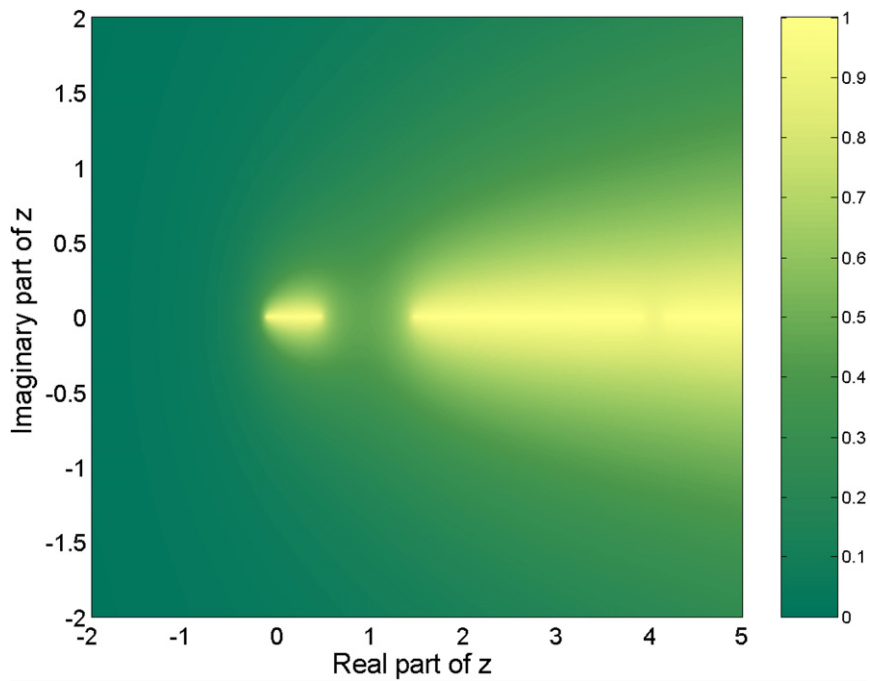


Fig. 3. Case C: Modulus of  $\sigma$  with respect to  $z$ .

$$I_{SE}(z) = -\sqrt{-z + a_1} \prod_{r=1}^{+\infty} \frac{\sqrt{-z + a_{r+1}}}{\sqrt{-z + b_r}}, \quad \text{Im} z > 0,$$

where  $\sqrt{\cdot}$  denotes the branch of the square root with positive real part.

The branch cut is set as the negative real axis. Intensive numerical tests in [29] verified the validity of this formula. Since formally  $I_{SE}(\bar{z}) = \overline{I_{SE}(z)}$  for any  $z$  with  $\text{Im}z \neq 0$ , it is thus tempting to generalize the above conjecture to our general second-order ODE (2), i.e.,

$$I(z) = -\sqrt{m(0)\rho(0)} \sqrt[+]{-z + a_1} \prod_{r=1}^{+\infty} \frac{\sqrt[+]{-z + a_{r+1}}}{\sqrt[+]{-z + b_r}}, \quad \text{Im}z \neq 0. \quad (9)$$

**Remark 2.** For a better understanding of the impedance condition (9) let us discuss how to obtain the constant coefficient case from the more general formula (9). The impedance for constant coefficients is given by

$$I(z) = -\sqrt{m\rho} \sqrt[+]{-z + \frac{V}{\rho}} = -\sqrt[+]{m(V - \rho z)}.$$

All the eigenvalues of (8) are

$$\lambda_n = \frac{\left(\frac{n\pi}{S}\right)^2 + mV}{m\rho}.$$

The eigenspace of  $\lambda_0$  is the set of constant functions. For  $n > 0$ , the eigenvalue  $\lambda_n$  is degenerate. Its eigenspace is two-dimensional, spanned by  $\cos(\pi x/S)$  and  $\sin(\pi x/S)$ . Notice that  $\cos$  is even and  $\sin$  is odd.

Thus we have

$$a_n = \lambda_{n-1}, \quad n \geq 1 \quad \text{and} \quad b_n = \lambda_n, \quad n \geq 1.$$

Since  $a_{r+1} = b_r$  for any  $r \geq 1$ , Eq. (9) yields

$$I = -\sqrt{m\rho} \sqrt[+]{-z + a_1} = -\sqrt[+]{m(V - \rho z)},$$

the correct impedance expression.

Let us consider another two numerical tests:

$$\text{Case D:} \quad m(x) = \rho(x) = 1, \quad V(x) = \sum_{n=-\infty}^{+\infty} e^{-16(x-\pi/2-n\pi)^2},$$

$$\text{Case E:} \quad m(x) = 1, \quad V(x) = 0, \quad \rho(x) = 1 + \cos(2x)/5.$$

Case D corresponds to the Schrödinger equation with a periodic Gaussian potential, cf. Fig. 4, and Case E could arise from a second-order hyperbolic wave equation in a periodic medium.

Figs. 5 and 6 show the impedance function  $I(z)$  when  $z$  is very close to the real axis. It can be clearly seen that the impedance turns out to be either real or purely imaginary. Those real intervals with purely imaginary impedance are exactly those values of  $z$  for which the ODE (2) has no nontrivial  $L^2$ -solution. In the engineering literature these intervals are called *pass bands*, while their complementary intervals are called *stop bands*. Several remarks have to be made at this point.

**Remark 3.** The impedance  $I(z)$  becomes much more complicated as  $z$  approaches the real axis if one of the coefficient functions  $m(x)$ ,  $V(x)$  and  $\rho(x)$  is not centrally symmetric, cf. (3).

**Remark 4.** The eigenvalues  $a_r$  and  $b_r$  can be computed with a high-accuracy solver for the characteristic problem (8). The first few eigenvalues are listed in Tables 1 and 2 with 6 digits. We observe that the relative difference between  $a_{r+1}$  and  $b_r$  decays very fast when  $r$  increases.

**Remark 5.** If the coefficient functions  $m(x)$  and  $\rho(x)$  are constant and  $V(x) = 2q \cos(2x)$  with  $q > 0$ , then the general ODE (2) is reduced to the well-known *Mathieu's equation* [3,19]. In this case, we obtain

$$a_1 < b_1 < a_2 < b_2 < a_3 < b_3 < \dots$$

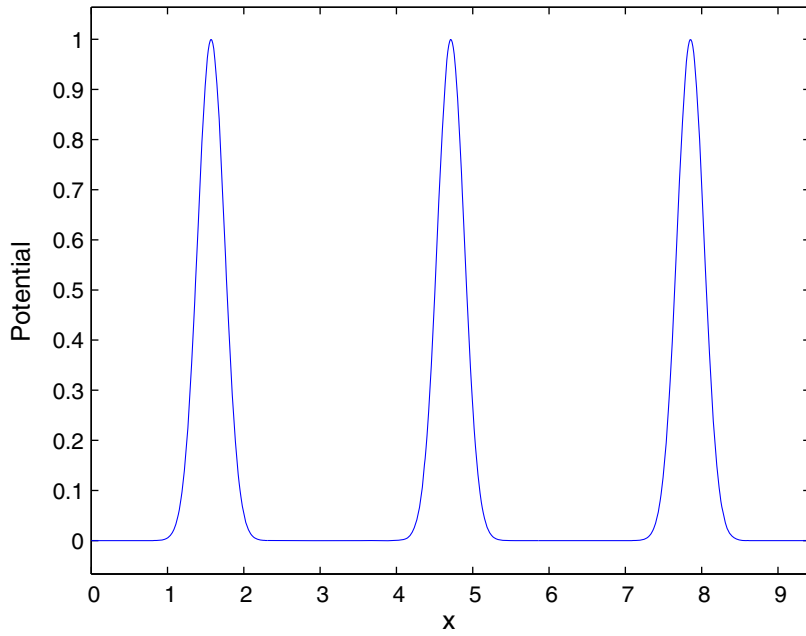
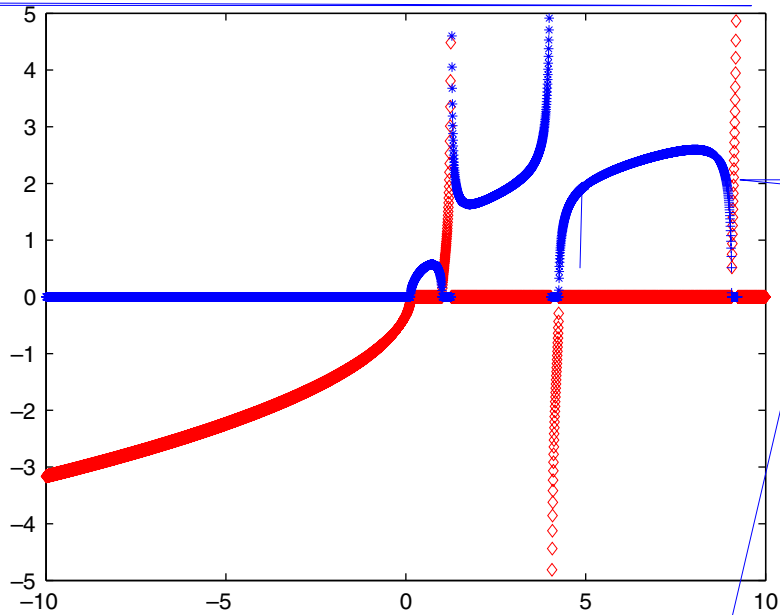


Fig. 4. Periodic Gaussian potential function  $V(x) = \sum_{n=-\infty}^{+\infty} e^{-16(x-\pi/2-n\pi)^2}$ .



However, in general this property does not hold, and we can only expect the following

$$a_1 < \min(a_2, b_1) \leq \max(a_2, b_1) < \min(a_3, b_2) \leq \max(a_3, b_2) < \dots$$

**Remark 6.** The stop bands are characterized as

$$(-\infty, a_1), (\min(a_2, b_1), \max(a_2, b_1)), (\min(a_3, b_2), \max(a_3, b_2)), \dots$$

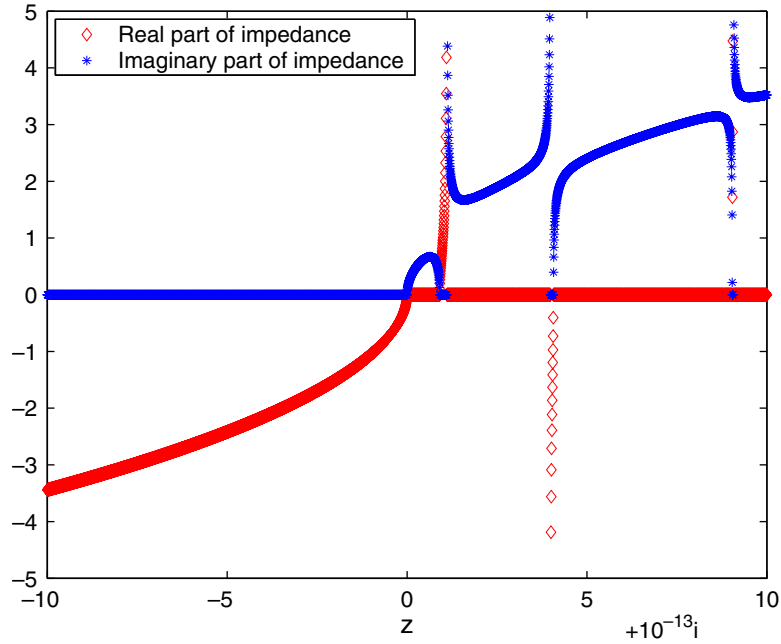


Fig. 6. Case E: Impedance plot for  $m = 1$ ,  $V = 0$  and  $\rho = 1 + \cos(2x)/5$ .

and the pass bands are given by

$$(a_1, \min(a_2, b_1)), (\max(a_2, b_1), \min(a_3, b_2)), (\max(a_3, b_2), \min(a_4, b_3)), \dots$$

Now let us consider the expression (9) with the infinite product limited to  $R$  factors:

$$I_R(z) = -\sqrt{m(0)\rho(0)} \sqrt[3]{-z + a_1} \prod_{r=1}^R \frac{\sqrt[3]{-z + a_{r+1}}}{\sqrt[3]{-z + b_r}}, \quad \text{Im } z \neq 0. \tag{10}$$

Figs. 7 and 8 show the maximum errors between the impedance  $I(z)$  and  $I_R(z)$  on 4001 equidistant points on three segments of the upper half complex plane. We detect that these errors become very small with increasing

Table 1

Case D: The first several eigenvalues of (8) with  $m(x) = \rho(x) = 1$  and  $V(x) = \sum_{n=-\infty}^{+\infty} e^{-16(x-\pi/2-n\pi)^2}$

$r$	$a_{r+1}$	$b_r$	$r$	$a_{r+1}$	$b_r$	$r$	$a_{r+1}$	$b_r$
0	1.30811(-1)		5	2.51111(1)	2.51730(1)	10	1.00142(2)	1.00141(2)
1	1.00842(0)	1.26431(0)	6	3.61574(1)	3.61260(1)	11	1.21141(2)	1.21141(2)
2	4.25428(0)	4.03081(0)	7	4.91344(1)	4.91486(1)	12	1.44141(2)	1.44141(2)
3	9.06010(0)	9.22586(0)	8	6.41442(1)	6.41386(1)	13	1.69141(2)	1.69141(2)
4	1.61965(1)	1.60886(1)	9	8.11403(1)	8.11423(1)	14	1.96141(2)	1.96141(2)

Table 2

Case E: The first few eigenvalues of (8), where  $m(x) = 1$ ,  $V(x) = 0$  and  $\rho(x) = 1 + \cos(2x)/5$

$r$	$a_{r+1}$	$b_r$	$r$	$a_{r+1}$	$b_r$	$r$	$a_{r+1}$	$b_r$
1	9.08164(-1)	1.10938	5	2.51315(1)	2.51328(1)	9	8.14157(1)	8.14157(1)
2	4.06748	3.98676	6	3.61880(1)	3.61877(1)	10	1.00512(2)	1.00512(2)
3	9.04010	9.06316	7	4.92536(1)	4.92537(1)	11	1.21618(2)	1.21618(2)
4	1.60896(1)	1.60838(1)	8	6.43296(1)	6.43296(1)	12	1.44735(2)	1.44735(2)

Notice that  $a_1 = 0$ .



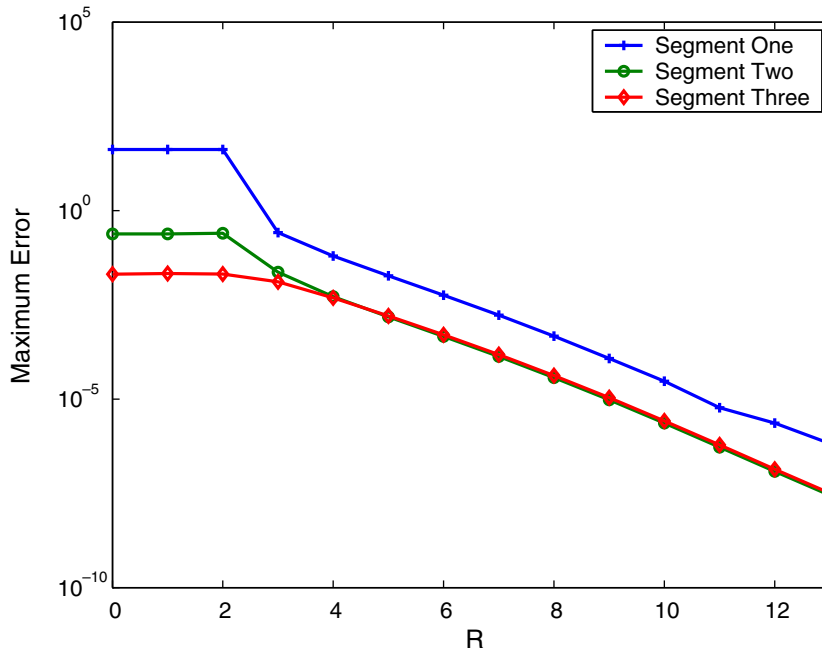


Fig. 7. Case D: Maximum error between the impedance  $I(z)$  and  $I_R(z)$ . Segment one:  $[-10, 10] + 10^{-13}i$ . Segment two:  $[-10, 10] + i$ . Segment three:  $[-10, 10] + 10i$ .

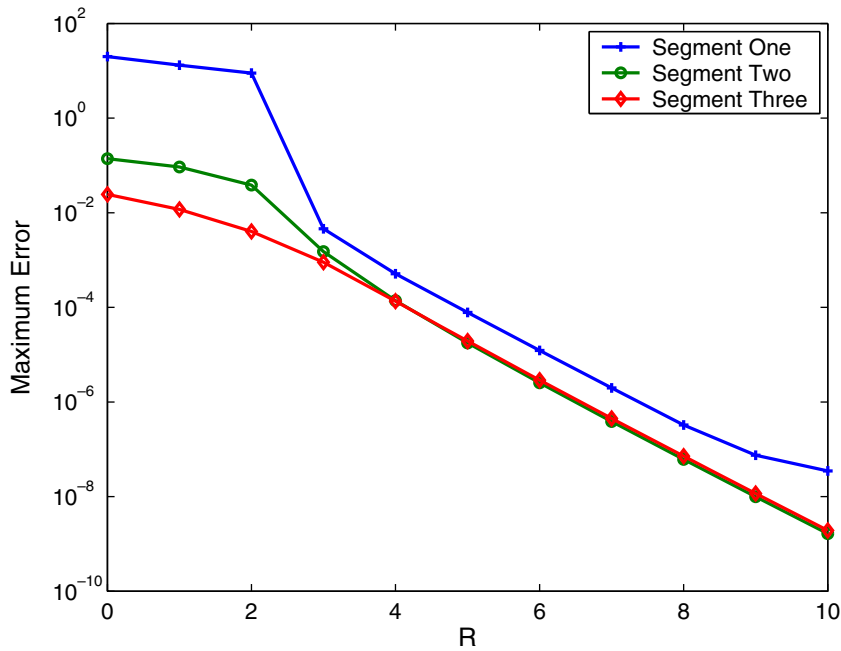


Fig. 8. Case E: Maximum error between the impedance  $I(z)$  and  $I_R(z)$ . Segment one:  $[-10, 10] + 10^{-13}i$ . Segment two:  $[-10, 10] + i$ . Segment three:  $[-10, 10] + 10i$ .

$R$ . This observation has also been made for many other numerical tests. It is thus reasonable to conjecture that the limit of  $I_R(z)$  as  $R$  tends to  $+\infty$  is the impedance  $I(z)$ , i.e. the formula (9) states the correct impedance expression.

Let us note that we are trying to prove conjecture presented above, namely if the potential is centrally symmetric, then (9) gives the analytical expression of the impedance operator. The proofs will rely on the theory on so-called *boundary triplets* and the analysis of the associated (Titchmarsh-) Weyl functions and it will be a generalization of the two recent works [5,6].

If  $z = z_0$  is a real number, then the impedance expression (9) might not be well-defined. If  $z_0$  lies in one of the stop bands, we already know that

$$\lim_{\epsilon \rightarrow 0^+} \operatorname{Im} I(z_0 + \epsilon) = 0.$$

Due to the symmetry property of the impedance, i.e.  $I(\bar{z}) = \overline{I(z)}$ , we can define

$$I(z_0) = \lim_{\epsilon \rightarrow 0^+} I(z_0 \pm \epsilon).$$

Hence the impedance expression (9) still can be considered valid. If  $z_0$  lies in one of the pass bands, the ODE (2) has no nontrivial bounded  $L^2$ -solution. In this case, we have to specify what kind of solution is really what we are seeking for. The impedance of this solution is thus the one-sided limit of  $I(z_0 + \epsilon)$  as either  $\epsilon \rightarrow 0^+$  or  $\epsilon \rightarrow 0^-$ . In most cases, this choice can be made naturally under physical considerations.

### 3. Bound states for the Schrödinger operator

As a first application of the impedance expression (9), we consider the following *bound state problem for the Schrödinger operator*:

Find an energy  $E \in \mathbb{R}$  and a nontrivial real function  $u \in L^2(\mathbb{R})$ , such that

$$-\frac{d^2 u}{dx^2} + V(x)u = Eu, \quad x \in \mathbb{R}, \quad (11)$$

where

$$V(x) = \begin{cases} 2 + 2 \cos(\pi x), & |x| > 1, \\ 0, & |x| < 1. \end{cases}$$

The potential function  $V(x)$  is periodic in  $\mathbb{R} \setminus (-1, 1)$ . In order to ensure that the solution  $u$  has a bounded  $L^2$ -norm, the energy  $E$  must be valued in the stop bands. The first few eigenvalues of the characteristic problem (8) with  $m(x) = \rho(x) = 1$  and  $V(x) = 2 - 2 \cos(\pi x)$  (NOT  $V(x) = 2 + 2 \cos(\pi x)$ ) are listed in Table 3.

The first three stop bands are given by

$$(-\infty, 1.80087), (3.41926, 5.41414), (11.8359, 12.0349).$$

If  $E$  is a bound state energy, then it must be an eigenvalue of the following *nonlinear characteristic problem*:

Find an energy  $E \in \mathbb{R}$  and a nontrivial real function  $u \in L^2(-1, 1)$ , such that

$$-\frac{d^2 u}{dx^2} + V(x)u = Eu, \quad x \in (-1, 1), \quad (12a)$$

$$-\frac{du}{dx}(-1) = I(E)u(-1), \quad (12b)$$

$$\frac{du}{dx}(1) = I(E)u(1). \quad (12c)$$

Table 3

The first few eigenvalues of (8) with  $m(x) = \rho(x) = 1$  and  $V = 2 - 2 \cos(\pi x)$

$r$	$a_{r+1}$	$b_r$	$r$	$a_{r+1}$	$b_r$
0	1.80087		3	2.42294(1)	2.42345(1)
1	3.41926	5.41414	4	4.14920(1)	4.14919(1)
2	1.20349(1)	1.18359(1)	5	6.36935(1)	6.36935(1)

A direct discretization of the above problem (12) leads to a very complicated nonlinear algebraic equation with respect to  $E$ , and its solvability is not completely clear. Actually, the problem (12) is equivalent to the following *fixed point problem*. For a given energy  $E$  we can solve the *linear characteristic problem*:

Find a function  $\Phi(E) \in \mathbb{R}$  and a nontrivial real function  $u \in L^2(-1, 1)$ , such that

$$-u_{xx} + V(x)u = \Phi(E)u, \quad x \in (-1, 1), \tag{13a}$$

$$-\frac{du}{dx}(-1) = I(E)u(-1), \tag{13b}$$

$$\frac{du}{dx}(1) = I(E)u(1). \tag{13c}$$

The bound state energy thus satisfies  $E = \Phi(E)$ , i.e.  $E$  is a fixed point of the function  $\Phi(E)$ . Notice that  $\Phi(E)$  is a multi-valued function and hence a series of bound states are expected.

Fig. 9 shows the first three branches of  $\Phi(E)$  being restricted to  $[-8, 15]$ . The time-harmonic Schrödinger equation is discretized by 50 eighth-order finite elements in  $[-1, 1]$ .  $I(E)$  is approximated by  $I_{14}(E)$ , which is equal to  $I(E)$  within machine precision if  $|E| < 20$ . Three bound states exist in this energy range. By performing the Newton–Steffenson iterations, the energies are found to be  $E_0 = 0.642647$ ,  $E_1 = 4.88651$  and  $E_2 = 12.0164$ . Our computations show that these values do not change within 6 digits by refining the finite element mesh.

The bound state wave functions (not normalized) are plotted in Fig. 10. We observe in Fig. 10 that the ground state is well-localized, while the second excited bound state is greatly delocalized. This demonstrates the advantage of the artificial boundary method and especially our ABCs (13b) and (13c), since a direct domain truncation method necessitates a very large computational domain to ensure the approximating accuracy of the wave function.

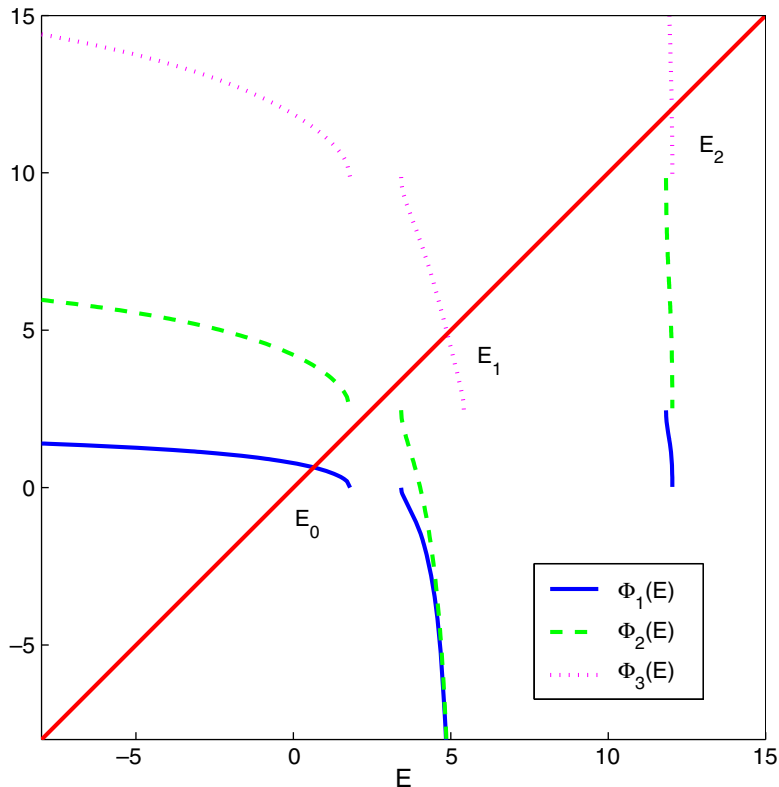
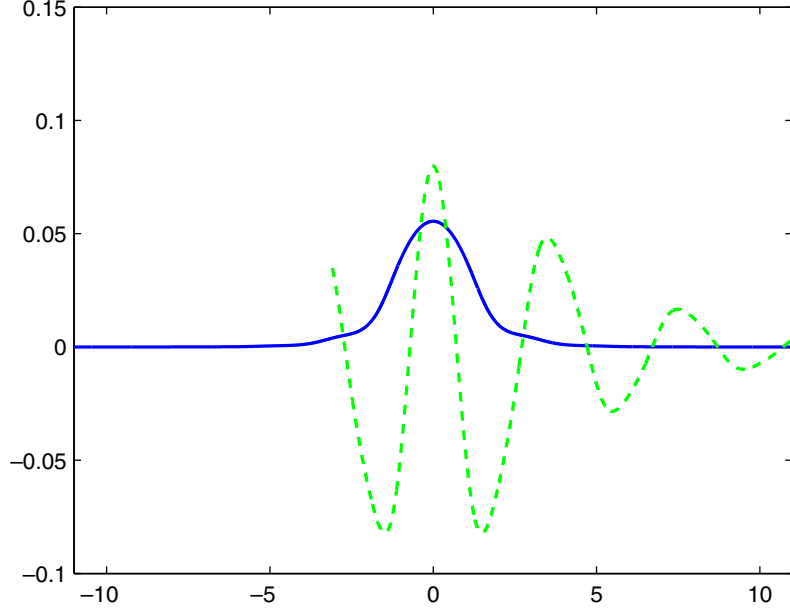


Fig. 9.  $E_0 = 0.642647(-1)$ .  $E_1 = 4.88651$ .  $E_2 = 12.0164(1)$ .



#### 4. Exact artificial boundary conditions for time-dependent problems

Based on the fundamental impedance expression (9), exact artificial boundary conditions can be derived for many time-dependent periodic structure problems, e.g., the Schrödinger equation (SE)

$$i\rho(x)\frac{\partial u}{\partial t} + \frac{\partial}{\partial x}\left(\frac{1}{m(x)}\frac{\partial u}{\partial x}\right) = V(x)u,$$

the diffusion equation (DE)

$$\rho(x)\frac{\partial u}{\partial t} = \frac{\partial}{\partial x}\left(\frac{1}{m(x)}\frac{\partial u}{\partial x}\right) - L(x)u,$$

and the second-order hyperbolic equation (HE)

$$\frac{\partial}{\partial x}\left(\frac{1}{m(x)}\frac{\partial u}{\partial x}\right) - L(x)u = \rho(x)\frac{\partial^2 u}{\partial t^2}.$$

Here, the coefficients  $V(x)$ ,  $\rho(x)$ ,  $m(x)$  and  $L(x)$  are supposed to be centrally symmetric periodic functions at infinity. Moreover,  $\rho(x)$  and  $m(x)$  are positive, and  $L(x)$  is nonnegative. The impedances for these three equations are given by

$$I_{SE}(is) = -\sqrt{m(0)\rho(0)}\sqrt[4]{-is + a_1} \prod_{r=1}^{+\infty} \frac{\sqrt[4]{-is + a_{r+1}}}{\sqrt[4]{-is + b_r}}, \quad (14)$$

and

$$I_{DE}(-s) = -\sqrt{m(0)\rho(0)}\sqrt[4]{s + a_1} \prod_{r=1}^{+\infty} \frac{\sqrt[4]{s + a_{r+1}}}{\sqrt[4]{s + b_r}}, \quad (15)$$

and

$$I_{HE}(-s^2) = -\sqrt{m(0)\rho(0)}\sqrt[4]{s^2 + a_1} \prod_{r=1}^{+\infty} \frac{\sqrt[4]{s^2 + a_{r+1}}}{\sqrt[4]{s^2 + b_r}}. \quad (16)$$

In Eqs. (14)–(16) the variable  $s$  with  $\text{Re } s > 0$  denotes the free argument in the Laplace domain. Notice that due to our assumption, all coefficients  $a_r$  and  $b_r$  in (15) and (16) are nonnegative and thus the formulas (15) and (16) are well-defined. The numerical solution to the Schrödinger equation in conjunction with the ABC (14) has been investigated in [29]. Similar techniques can be used for the diffusion equation with the ABC (15) with minor modifications. In the sequel we will focus on a second-order hyperbolic equation in a two-dimensional setting.

To do so, we consider the propagation of electromagnetic waves in a waveguide with cavity, cf. the schematic map Fig. 11. For a TM polarized electromagnetic wave, the electric field  $E$  is governed by the equation

$$\frac{\partial^2 E}{\partial x^2} + \frac{\partial^2 E}{\partial z^2} - \frac{\epsilon(x, z)}{c^2} \frac{\partial^2 E}{\partial t^2} = 0. \tag{17}$$

The relative dielectric permittivity  $\epsilon$ , depending only on  $x$  after the artificial boundary, is supposed to be periodic. We assume that this waveguide is enclosed with a perfect conductor and hence we have a homogeneous Dirichlet boundary condition  $E = 0$  on the physical boundary.

On the semi-infinite slab region  $[0, +\infty) \times [0, 1]$ , the characteristic decomposition can be applied with respect to the  $z$  variable. The eigenvalues are given by  $n^2\pi^2$  and the eigenfunctions are  $\sin(n\pi z)$ ,  $n \geq 1$ . An exact ABC in the frequency domain is thus set up as

$$\widehat{E}_x^n(0, s) = -\frac{\sqrt{\epsilon(0)}}{c} \sqrt{s^2 + a_1^n} \prod_{r=1}^{\infty} \frac{\sqrt{s^2 + a_{r+1}^n}}{\sqrt{s^2 + b_r^n}} \widehat{E}^n(0, s), \quad n \geq 1. \tag{18}$$

Here,  $\widehat{E}^n(x, s)$  denotes the  $n$ th mode of  $\widehat{E}(x, z, s)$  in the  $z$ -direction defined as

$$\widehat{E}^n(x, s) = 2 \int_0^1 \widehat{E}(x, z, s) \sin(n\pi z) dz, \quad x \geq 0, \quad n \geq 1.$$

$\widehat{E}(x, z, s)$  is determined by  $\widehat{E}^n(x, s)$  as

$$\widehat{E}(x, z, s) = \sum_{n=1}^{+\infty} \widehat{E}^n(x, s) \sin(n\pi z), \quad x \geq 0.$$

The constants  $a_r^n$  and  $b_r^n$  in (18) are the eigenvalues of the characteristic problem (8) with the coefficients  $m(x) = 1$ ,  $V(x) = n^2\pi^2$  and  $\rho(x) = \epsilon(x)/c^2$ . By setting

$$\widehat{w}_k^n(s) = \prod_{r=k}^{\infty} \frac{\sqrt{s^2 + a_{r+1}^n}}{\sqrt{s^2 + b_r^n}} \widehat{E}^n(0, s), \quad k \geq 1, \quad n \geq 1,$$

we obtain the recursion relation

$$\sqrt{s^2 + b_k^n} \widehat{w}_k^n(s) = \sqrt{s^2 + a_{k+1}^n} \widehat{w}_{k+1}^n(s), \quad k \geq 1, \quad n \geq 1,$$

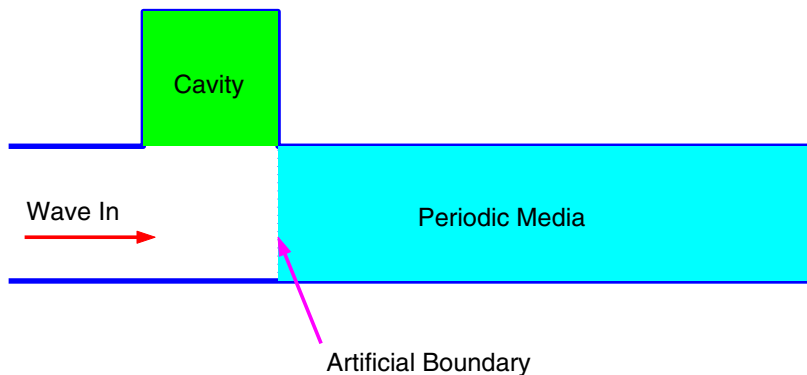


Fig. 11. Schematic map of a waveguide with cavity.

and (18) reads

$$\widehat{E}_x^n(0, s) = -\frac{\sqrt{\epsilon(0)}}{c} \sqrt{s^2 + a_1^n} \widehat{w}_1^n(s), \quad n \geq 1. \tag{19}$$

Now going back to the physical domain yields

$$\frac{dw_k^n}{dt} = \frac{dw_{k+1}^n}{dt} + \frac{\sqrt{a_{k+1}^n} J_1(\sqrt{a_{k+1}^n} t)}{t} * w_{k+1}^n - \frac{\sqrt{b_k^n} J_1(\sqrt{b_k^n} t)}{t} * w_k^n, \quad k \geq 1, \quad n \geq 0,$$

and from (19) we get

$$\begin{aligned} \frac{\partial E^n}{\partial x}(0, t) &= -\frac{\sqrt{\epsilon(0)}}{c} \left( \frac{dw_1^n}{dt} + \frac{\sqrt{a_1^n} J_1(\sqrt{a_1^n} t)}{t} * w_1^n \right) \\ &= -\frac{\sqrt{\epsilon(0)}}{c} \left( \frac{\partial E^n}{\partial t}(0, t) + \sum_{k=0}^{+\infty} \frac{\sqrt{a_{k+1}^n} J_1(\sqrt{a_{k+1}^n} t)}{t} * w_{k+1}^n - \sum_{k=1}^{+\infty} \frac{\sqrt{b_k^n} J_1(\sqrt{b_k^n} t)}{t} * w_k^n \right). \end{aligned} \tag{20}$$

Here, \* denotes a convolution with respect to the time variable  $t$  and  $J_1$  is the Bessel function of first order. In a real implementation the infinite summation terms in (20) have to be truncated. By simply keeping the first  $K_n$  terms we obtain

$$\frac{\partial E^n}{\partial x}(0, t) = -\frac{\sqrt{\epsilon(0)}}{c} \left( \frac{\partial E^n}{\partial t}(0, t) + \sum_{k=0}^{K_n} \frac{\sqrt{a_{k+1}^n} J_1(\sqrt{a_{k+1}^n} t)}{t} * w_{k+1}^n - \sum_{k=1}^{K_n} \frac{\sqrt{b_k^n} J_1(\sqrt{b_k^n} t)}{t} * w_k^n \right), \tag{21}$$

and

$$w_{K_n+1}^n(t) = E^n(0, t).$$

If we want to resolve the  $n$ th mode in the  $z$ -direction, we typically set  $K_n \geq 0$ . In order to ensure the approximating accuracy of the ABC,  $K_n$  should be increased for larger values of  $n$ . Of course, if we are not interested in the  $n$ th mode at all, we only need to set  $K_n = -1$ . In the following numerical example, we simply set  $K_n = 10$  for any  $n = 0, 1, \dots, N$ , and  $K_n = -1$  for any  $n = N + 1, \dots$ , where  $N$  denotes the number of modes in the  $z$ -direction we want to resolve.

**Numerical Example.** We now study the wave field generated by a *periodic disturbance* at the left physical boundary

$$E(-2, z, t) = \sin(\pi z) \sum_{n=0}^{+\infty} e^{-160(t-(n+0.5))^2}, \quad z \in (0, 1).$$

The wave speed is set to 1, and the dielectric permittivity  $\epsilon$  is set to be

$$\epsilon(x, z) = \begin{cases} 1, & x < 0, \\ 1.2 - 0.2 \cos(2\pi x), & x > 0. \end{cases}$$

We limit our computational time interval to  $[0, 6]$ . Due to the finite wave propagation speed (at most 1), we can compute a *reference solution*  $E_{\text{ref}}$  in a large domain  $(-2, 4) \times (0, 1) \cup (-1, 0) \times (1, 2)$  with small mesh sizes  $\Delta x = \Delta z = 0.00125$  and  $\Delta t = 0.000625$ . The leap-frog central difference scheme is employed in all the computations. We use the standard *fast evaluation technique* proposed by Alpert et al. [1,28] for the convolution operations involved in the ABC (21). The poles and weights are taken from the webpage of Hagstrom. The relative  $L^2$ -error is defined as

$$\frac{\|E_{\text{ref}}(\cdot, \cdot, t) - E_{\text{num}}(\cdot, \cdot, t)\|_{L^2}}{\|E_{\text{ref}}(\cdot, \cdot, 6)\|_{L^2}},$$

where  $E_{\text{ref}}$  stands for the reference solution, while  $E_{\text{num}}$  denotes the numerical solution.

In Figs. 12 and 13 we compare the numerical solutions with the reference solutions at two different time steps. No difference can be observed with eyes.

In Fig. 14 we depict the errors when different number of modes in the  $z$ -direction are used. The accuracy of the numerical solutions is greatly improved for large number of modes.

The error evolution with respect to the time  $t$  is shown in Fig. 15. At the initial stage, the wave does not reach the artificial boundary, thus the ABC has no influence on the numerical solutions. The error arises completely from the interior discretization. After a critical time point (almost  $t = 2.5$ ), the artificial boundary

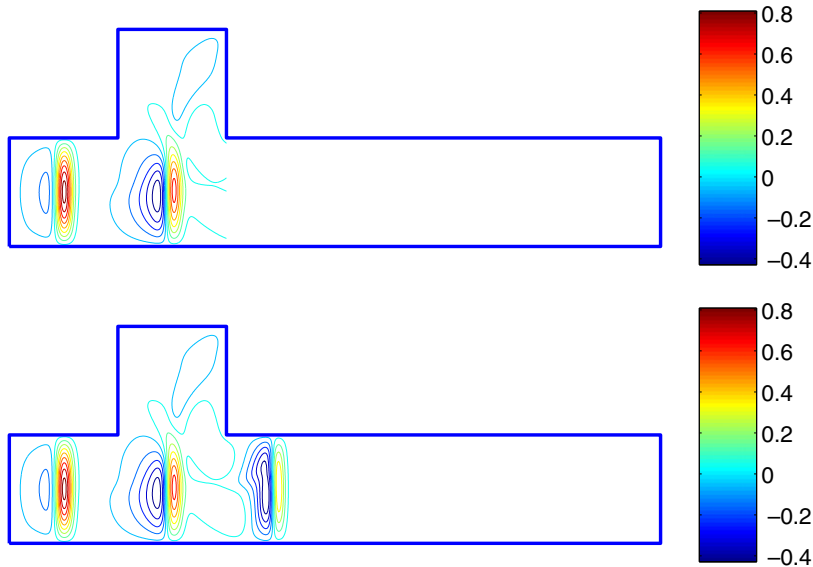


Fig. 12. At time  $t = 3$ . The number of modes is 10. The contour lines are  $-1 : 2/21 : 1$ .  $\Delta x = \Delta z = 0.005$ ,  $\Delta t = 0.0025$ . The reference solution is obtained by taking  $\Delta x = \Delta z = 0.00125$  and  $\Delta t = 0.000625$ .

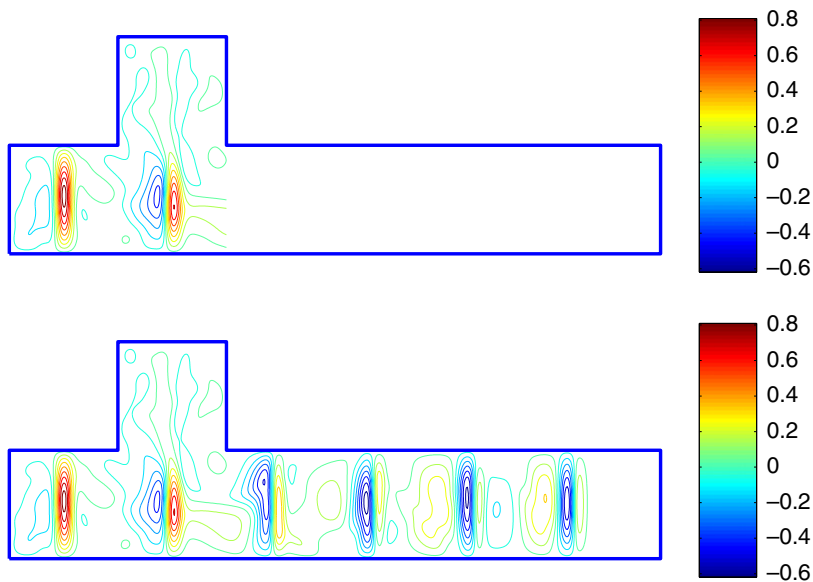


Fig. 13. At time  $t = 6$ . The number of modes is 10. The contour lines are  $-1 : 2/21 : 1$ .  $\Delta x = \Delta z = 0.005$ ,  $\Delta t = 0.0025$ . The reference solution is obtained by taking  $\Delta x = \Delta z = 0.00125$  and  $\Delta t = 0.000625$ .

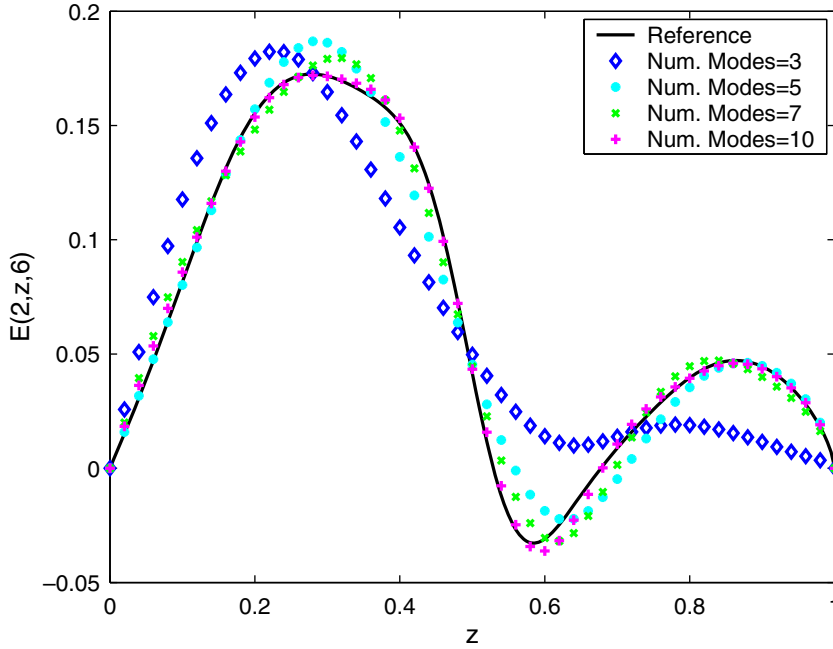


Fig. 14. At time  $t = 6$ ,  $\Delta x = \Delta z = 0.02$ ,  $\Delta t = 0.01$ . The reference solution is obtained by taking  $\Delta x = \Delta z = 0.00125$  and  $\Delta t = 0.000625$ . The line is  $x = 0$ .

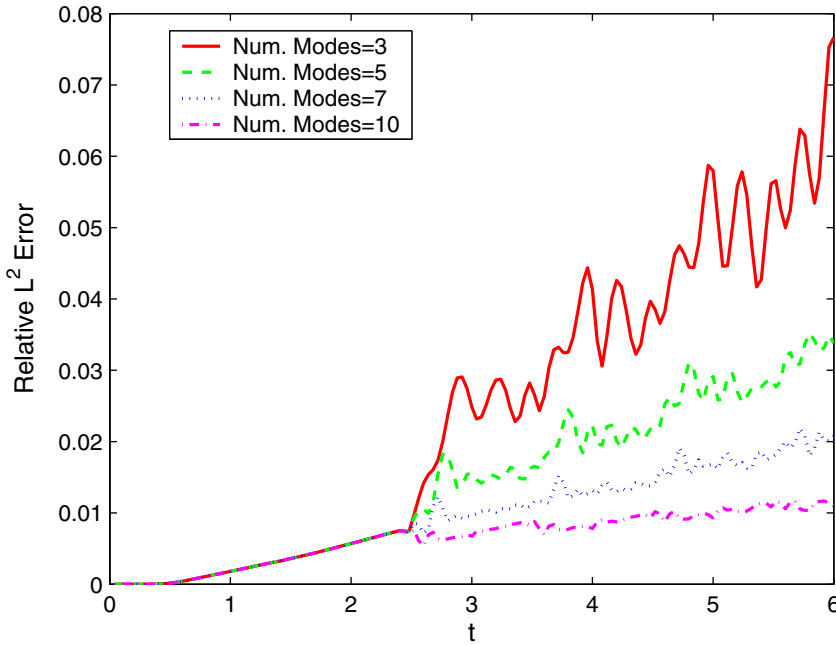


Fig. 15. Relative  $L^2$  error.  $\Delta x = \Delta z = 0.005$ ,  $\Delta t = 0.0025$ . The reference solution is obtained by taking  $\Delta x = \Delta z = 0.00125$  and  $\Delta t = 0.000625$ .

condition comes into effect. We see that if enough number of modes are used, the error from the approximate boundary condition is nearly on the same level of interior discretization, which means the ABC is sufficiently accurate in this parameter regime. Finally, we analyzed numerically in Fig. 16 the convergence rate of the



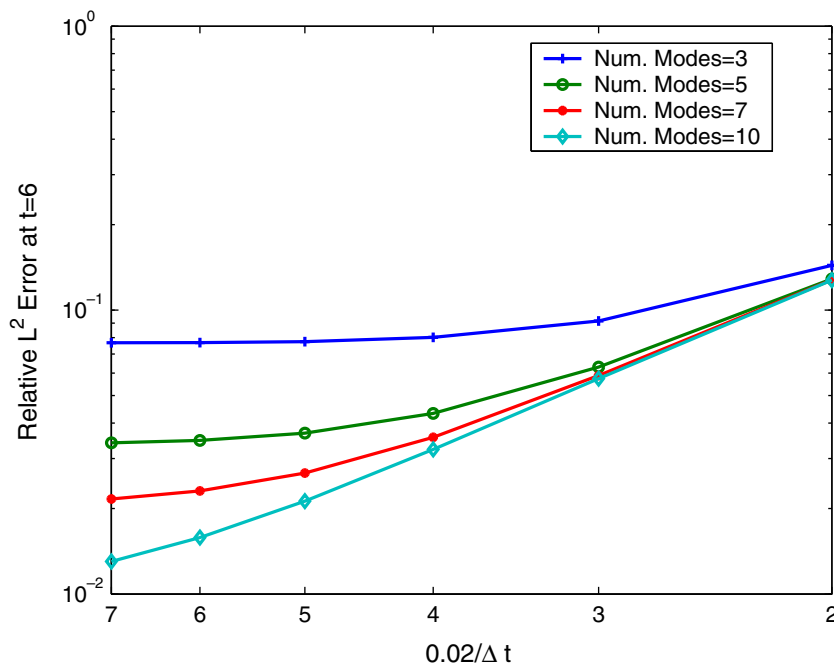


Fig. 16. Relative  $L^2$  error.  $\Delta x = \Delta z = 2\Delta t$ . The reference solution is obtained by taking  $\Delta x = \Delta z = 0.00125$  and  $\Delta t = 0.000625$ .

relative  $L^2$ -errors at  $t = 6$ . Data-fitting reveals that the errors decay with an order of 1.851 in the parameter range  $\Delta t \in [\frac{0.02}{7}, 0.01]$ , when the number of modes in the  $z$ -direction is set to 10.

## 5. Conclusions

In this paper we have generalized a recent result of Zheng [29] and derived an exact Dirichlet-to-Neumann artificial boundary condition for general problems with periodic structures at infinity. We considered in detail the bound state problem for the Schrödinger operator and a second-order hyperbolic equation in two space dimensions. Intensive numerical tests have strongly supported the validity of this new kernel expression for the artificial boundary condition, though at this stage we did not prove it theoretically, but the proof of this conjecture is currently under study.

It is tempting to generalize the result of this paper to the derivation of fully discrete artificial boundary conditions [7] for periodic potential problems. These boundary conditions are directly derived for the numerical scheme. Another very challenging task would be the extension of the present work to multi-dimensional problems with periodic structures.

## References

- [1] B. Alpert, L. Greengard, T. Hagstrom, Nonreflecting boundary conditions for the time-dependent wave equation, *J. Comput. Phys.* 180 (2002) 270–296.
- [2] X. Antoine, A. Arnold, C. Besse, M. Ehrhardt, A. Schädle, A Review of Transparent and Artificial Boundary Conditions Techniques for Linear and Nonlinear Schrödinger Equations, *Commun. Comput. Phys.* (2008).
- [3] F.M. Arscott, *Periodic Differential Equations*, Pergamon Press, Oxford, 1964.
- [4] G. Bastard, *Wave mechanics applied to semiconductor heterostructures*, les éditions de physique, Les Ulis Cedex, France, 1988.
- [5] J. Behrndt, M. Malamud, H. Neidhardt, Scattering theory for open quantum systems, WIAS-Berlin Preprint No. 1179.
- [6] J. Behrndt, M. Malamud, H. Neidhardt, Scattering matrices and Weyl functions, WIAS-Berlin Preprint No. 1121.
- [7] M. Ehrhardt, *Discrete Artificial Boundary Conditions*, Dissertation, TU Berlin, 2001.
- [8] S. Fliss, P. Joly, Exact boundary conditions for time-harmonic wave propagation in locally perturbed periodic media, *Appl. Numer. Math.*, 2008 (Special Issue of WONAPDE 2007: The Second Chilean Workshop on Numerical Analysis of Partial Differential Equations, Concepción, Chile, January 16–19, 2007).

- [9] C. Fox, V. Oleinik, B. Pavlov, A Dirichlet-to-Neumann map approach to resonance gaps and bands of periodic networks, in: N. Chernov, Y. Karpeshina, I.W. Knowles, R.T. Lewis, R. Weikard (Eds.), *Recent Advances in Differential Equations and Mathematical Physics*, Contemp. Math., vol. 412, Amer. Math. Soc., Providence, RI, 2006, pp. 151–169.
- [10] H. Galicher, Transparent boundary condition for the one-dimensional Schrödinger equation with periodic potentials at infinity, *Commun. Math. Sci.* (submitted for publication).
- [11] D. Givoli, Non-reflecting boundary conditions, *J. Comput. Phys.* 94 (1991) 1–29.
- [12] T. Hagstrom, Radiation boundary conditions for the numerical simulation of waves, *Acta Numer.* 8 (1999) 47–106.
- [13] P. Joly, J.-R. Li, S. Fliss, Exact boundary conditions for periodic waveguides containing a local perturbation, *Commun. Comput. Phys.* 1 (2006) 945–973.
- [14] P. Kuchment, Floquet theory for partial differential equations, *Operator Theory: Advances and Applications*, vol. 60, Birkhäuser Verlag, Basel, 1993.
- [15] P. Kuchment, The mathematics of photonic crystals, in: *Mathematical Modeling in Optical Science*, *Frontiers in Applied Mathematics*, vol. 22, SIAM, Philadelphia, 2001 (Chapter 7).
- [16] J.S. Papadakis, Impedance formulation of the bottom boundary condition for the parabolic equation model in underwater acoustics, *NORDA Parabolic Equation Workshop*, *NORDA Tech. Note* 143, 1982.
- [17] A. Pazy, *Semigroups of Linear Operators and Applications to Partial Differential Equations*, Springer, New York, 1983.
- [18] M. Reed, B. Simon, *Methods of Modern Mathematical Physics II: Fourier Analysis, Self-adjointness*, Academic Press, San Diego, 1975.
- [19] J.A. Richards, *Analysis of Periodically Time-Varying Systems*, Springer-Verlag, 1983.
- [20] K. Sakoda, *Optical Properties of Photonic Crystals*, Springer-Verlag, Berlin, 2001.
- [21] I.A. Semenikhin, B.S. Pavlov, V.I. Ryzhii, Plasma waves in two-dimensional electron channels: propagation and trapped modes, Preprint No. NI07028-AGA of the Isaac Newton Institute for Mathematical Sciences, 2007.
- [22] J. Tausch, J. Butler, Floquet multipliers of periodic waveguides via Dirichlet-to-Neumann maps, *J. Comput. Phys.* 159 (2000) 90–102.
- [23] J. Tausch, J. Butler, Efficient analysis of periodic dielectric waveguides using Dirichlet-to-Neumann maps, *J. Opt. Soc. Am. A* 19 (2002) 1120–1128.
- [24] S.V. Tsynkov, Numerical solution of problems on unbounded domains. A review, *Appl. Numer. Math.* 27 (1998) 465–532.
- [25] A. Wacker, Semiconductor superlattices: a model system for nonlinear transport, *Phys. Rep.* 357 (2002) 1–111.
- [26] L. Yuan, Y.Y. Lu, Dirichlet-to-Neumann map method for second harmonic generation in piecewise uniform waveguides, *J. Opt. Soc. Am. B* 24 (2007) 2287–2293.
- [27] L. Yuan, Y.Y. Lu, A recursive doubling Dirichlet-to-Neumann map method for periodic waveguides, *J. Lightwave Technol.* 25 (2007) 3649–3656.
- [28] C. Zheng, Approximation, stability and fast evaluation of an exact artificial boundary condition for the one-dimensional heat equation, *J. Comput. Math.* 25 (2007) 730–745.
- [29] C. Zheng, An exact boundary condition for the Schrödinger equation with sinusoidal potentials at infinity, *Commun. Comput. Phys.* 3 (2007) 641–658.